



# Synthesis, characterization, computational studies and DPPH scavenging activity of some triazatetracyclic derivatives

F. Odame<sup>1,2</sup> · Eric C. Hosten<sup>2</sup> · R. Betz<sup>2</sup> · J. Krause<sup>3</sup> · Carminita L. Frost<sup>3</sup> · K. Lobb<sup>4</sup> · Zenixole R. Tshentu<sup>2</sup>

Received: 7 August 2020 / Accepted: 2 January 2021  
© Iranian Chemical Society 2021

## Abstract

Some dihydrobenzo[4,5]imidazo[1,2-c]quinazolines have been synthesized from aldehydes and ketones, using the ketones as both reagents and solvents and tetrahydrofuran (THF) as the solvent for the aldehydes, to yield the triazatetracyclics. The compounds have been characterized with spectroscopy and microanalysis. The crystal structures of 9,9-dimethyl-8,10,17-triazatetracyclo[8.7.0<sup>2,7</sup>.0<sup>11,16</sup>]heptadeca-1(17),2,4,6,11(16),12,14-heptaene (**I**), 9-butyl-9-methyl-8,10,17-triazatetracyclo[8.7.0.0<sup>2,7</sup>.0<sup>11,16</sup>]heptadeca-(17),2,4,6,11(16),12,14-heptaene (**III**) and 9-phenyl-8,10,17-triazatetracyclo[8.7.0.0<sup>2,7</sup>.0<sup>11,16</sup>]heptadeca-1(17),2,4,6,11(16),12,14-heptaene (**VIII**) have been discussed. The computed NMR, IR, molecular electrostatic potential and frontier molecular orbitals of compounds **I**, **III** and **VIII** have been discussed. The M06 functional gave most of its values closest to the experimental values for the bond lengths and bond angles of compounds **I** and **III**. For compound **VIII**, none of the functionals gave values for bond lengths and bond angles that were consistent with the experimental values, but M06 gave values closest to experimental values. The 1,1-diphenyl-2-picrylhydrazyl (DPPH) scavenging activity of the triazatetracyclics showed that compound **I** exhibits significant DPPH scavenging activity with an IC<sub>50</sub> of 56.18 μM compared to 2.37 μM for ascorbic acid.

**Keywords** Aminophenylbenzimidazole · Aldehydes · Ketones · Triazatetracyclics · Scavenging activity · Frontier orbitals

## Introduction

Benzimidazoles have attracted a lot of interest based on their biological activity [1–5]. Dihydrobenzo[4,5]imidazo[1,2-c]quinazolines provides a chemical scaffold on which different potentially bioactive tetracyclic compounds can be constructed. It is well known that amines undergo condensation reactions with aldehydes and ketones but utilization of this in the formation of cyclic amines often requires a more intricate synthetic procedure. Cyclic amines have been accessed

via a sequence of deprotection reactions followed by intermolecular reductive amination of *t*-Boc-protected amino ketones under asymmetric transfer hydrogenation conditions [6]. Cyclization of diamines and ketones has also been catalysed by HY zeolite at 50 °C under solvent-free conditions to give benzodiazepines [7]. Benzodiazepine formation has also been reported to occur in the absence of a catalyst [8]. A three-component allylation and cyanation reaction utilizing a ketone and *N*-methoxyamine have been reported, and the high nucleophilicity of the *N*-methoxyamine and high electrophilicity of the corresponding iminium ion facilitate the concise synthesis of trisubstituted amines in a single step [9]. A fourth method reported in the literature; the treatment of *N*-tosyl dimines with acetophenone at room temperature gave the corresponding *N*-tosyl β-amino ketones in high yields within 6–9 h. Subsequent reduction and cyclization of the compounds in this case afforded 2,4-disubstituted *N*-tosylazetidines, comprising a three step high yielding synthesis from aldimines [10].

Twelve *N*-glycosyl amines were synthesized using 4,6-*O*-benzylidene-*D*-glucopyranose and different substituted aromatic amines, including some diamines that

✉ F. Odame  
felixsah15@gmail.com

<sup>1</sup> University of Health and Allied Sciences, PMB 31, Ho, Ghana

<sup>2</sup> Department of Chemistry, Nelson Mandela University, P.O. Box 77000, Port Elizabeth 6031, South Africa

<sup>3</sup> Department of Biochemistry and Microbiology, Nelson Mandela University, P.O. Box 77000, Port Elizabeth 6031, South Africa

<sup>4</sup> Department of Chemistry, Rhodes University, P.O. Box 94, Grahamstown 6140, South Africa

resulted in bis-glycosyl amines. Another set of six *N*-glycosyl amines was synthesized using different hexoses and pentoses with 2-(*o*-aminophenyl)benzimidazole. In these reactions, only the 2-amino group reacted with the hydroxyl groups of 2-(*o*-aminophenyl)benzimidazole [11]. Reactions of substituted aldehydes with 2-(*o*-aminophenyl)benzimidazole have been reported to yield Schiff bases [12]. The syntheses of 2-(2-nitrophenyl)-1-benzoyl-1*H*-benzimidazole derivatives and their reduction to the corresponding 2-benzimidazolylbenzamides have been reported. The compounds were cleanly and efficiently converted to the corresponding 6-arylbenzimidazo[1,2-*c*]quinazolines by microwave activation using SiO<sub>2</sub>-MnO<sub>2</sub> as solid inorganic support [13]. In our case, the products were accessed via a solvent-free approach for the ketones, whilst tetrahydrofuran was used as a solvent for the aldehydes. Some triazatetracyclic compounds containing Schiff bases have been synthesized and characterized for their anti-proliferative properties and in-vitro cholinesterase inhibition [14]. The fluorescent properties of some triazatetracyclic compounds have been determined. The compounds showed high selectivity for Hg<sup>2+</sup> ions as ‘on-off’ switch [15].

Evaluation of the antioxidant activities of natural substances has been of interest in recent years. Antioxidants scavenge free radicals and reactive oxygen species; they can be extremely important in inhibiting oxidative mechanisms that lead to degenerative diseases [16]. Free radicals have been implicated as playing a role in cardiovascular disease, cancer, Alzheimer’s disease and Parkinson’s disease. The antioxidant capacity of a compound is usually associated with their phenolic content. Although plant polyphenols such as tannins and flavonoids have problems of astringency and protein binding making them anti-nutrients [17, 18], they have been found useful as natural antioxidants in scavenging deleterious free radicals released in the body by fat metabolism [19]. Some phenolic compounds have also been tested for their antioxidant activity [20–22].

Frontier orbitals are useful in predicting the most reactive position in  $\pi$ -electron systems and to explain several types of reactions in conjugated systems [23]. The conjugated molecules are characterized by a small Highest Occupied Molecular Orbital (HOMO) and Lowest Unoccupied Molecular Orbital (LUMO) separation, which is the result of a significant degree of intramolecular charge transfer from the end capping electron-donor groups through a  $\pi$ -conjugated path [24]. The HOMO and LUMO are the main orbitals that determine chemical stability of any species [25]. The HOMO represents the ability to donate an electron, whilst the LUMO represents the ability to accept an electron. The energy of the HOMO is directly related to the ionization potential, whilst the energy of the LUMO is related to the electron affinity. The energy difference between HOMO and LUMO orbitals, known as the energy gap, determines

the stability or reactivity of molecules [26]. The energy gap is a critical parameter in determining molecular electrical transport properties because it is a measure of electron conductivity [27]. The hardness of a molecule also corresponds to the gap between the HOMO–LUMO orbitals [28]. Large HOMO–LUMO gap indicates high stability and resistance to charge transfer; therefore, hard molecules have a large HOMO–LUMO gap.

In our study of the reactions of structurally diverse amines, we investigated how a sterically hindered amine would react with ketones and aldehydes. Herein, we report the synthesis of some triazatetracyclics is obtained from the condensation of aldehydes or ketones with 2-(2'-aminophenyl)-1*H*-benzimidazole and a discussion of the crystal structures of compounds **I**, **III** and **VIII**. The orbitals that contribute to the reactivity of the synthesized compounds has been discussed. The computed bond lengths, bond angles, <sup>1</sup>H NMR and <sup>13</sup>C NMR of compounds **I**, **III** and **VIII** have been discussed with experimental values. The molecular electrostatic potentials have been computed and the surfaces plotted for compounds **I–VIII**. The 1,1-diphenyl-2-picrylhydrazyl (DPPH) scavenging activity of the triazatetracyclic compounds have been discussed.

## Experimental

### Materials and method

Analytical grade reagents and solvents for synthesis such as 2-(2'-aminophenyl)-1*H*-benzimidazole, 2-butanone, 2-pentanone, 2-hexanone and isobutyraldehyde were obtained from Sigma-Aldrich (USA), whilst acetone, acetophenone, 4-methylbenzaldehyde, 4-methylcyclohexanone and benzaldehyde were obtained from Merck Chemicals (SA). The chemicals were used as received (i.e. without further purification). <sup>1</sup>H NMR and <sup>13</sup>C NMR spectra were recorded on a Bruker Avance AV 400 MHz spectrometer operating at 400 MHz for <sup>1</sup>H and 100 MHz for <sup>13</sup>C using dimethyl sulfoxide as solvent and tetramethylsilane as internal standard. Chemical shifts are expressed in ppm. FT–IR spectra were recorded on a Bruker Platinum ATR Spectrophotometer Tensor 27. Microanalysis was performed using a Vario Elementar Microcube ELIII. Melting points were obtained using a Stuart Lasec SMP30, whilst the masses were determined using an Agilent 7890A GC System connected to a 5975C VL-MS-C with electron impact as the ionization mode and detection by a triple-Axis detector. The GC was fitted with a 30 m × 0.25 mm × 0.25  $\mu$ m DB-5 capillary column. Helium was used as carrier gas at a flow rate of 1.63 mL min<sup>-1</sup> with an average velocity of 30.16 cm s<sup>-1</sup> and a pressure of 63.73 kPa.

**9,9-Dimethyl-8,10,17-triazatetracyclo[8.7.0<sup>2,7</sup>.0<sup>11,16</sup>]heptadeca-1(17),2,4,6,11(16),12,14-heptaene (I)**

2-(2'-Aminophenyl)-1*H*-benzimidazole (0.015 mol) was heated under reflux in acetone (10 mL) for 6 h. The solvent was removed by rotary evaporation to obtain a yellow solid which was recrystallized as a yellow crystal from DMSO/toluene (1:1), yield = (2.89 g) 77.45%; mp = 209–211 °C. IR ( $\nu_{\max}$ ,  $\text{cm}^{-1}$ ): 3221 (N–H), 2956 (C–H), 1582 (C=N), 1513 (C=C), 1477 (C–N). <sup>1</sup>H NMR (400 MHz)  $\delta$  (ppm): 8.12–8.10 (m, 1H, Ar–H), 7.93 (d,  $J$  = 8.0 Hz, 1H, Ar–H), 7.83 (d,  $J$  = 6.4 Hz, 1H, Ar–H), 7.62–7.53 (m, 2H, Ar–H), 7.49 (t,  $J$  = 7.6, 8.4 Hz, 1H, Ar–H), 6.97–6.90 (m, 2H, Ar–H), 2.00 (s, 6H). <sup>13</sup>C NMR (100 MHz)  $\delta$  (ppm): 144.7 (C), 144.3 (C), 135.3 (CH), 125.2 (CH), 118.3 (CH), 114.6 (CH), 74.4 (C), 28.0 (CH<sub>3</sub>). Anal. calcd. for C<sub>16</sub>H<sub>15</sub>N<sub>3</sub>: C, 77.08; H, 6.06; N, 16.85. Found: C, 77.24; H, 6.13; N, 16.89. GC–MS ( $m/z$ , M<sup>+</sup>): Found for C<sub>16</sub>H<sub>15</sub>N<sub>3</sub> = 249.20, expected mass = 249.31.

**9-Ethyl-9-methyl-8,10,17-triazatetracyclo[8.7.0<sup>2,7</sup>.0<sup>11,16</sup>]heptadeca-1(17),2,4,6,11(16),12,14-heptaene (II)**

2-(2'-Aminophenyl)-1*H*-benzimidazole (0.015 mol) was heated under reflux in 2-butanone (10 mL) for 6 h. The solvent was removed by rotary evaporation to obtain a white solid which was recrystallized as a white crystal from DMSO/toluene (1:1), yield = (3.39 g) 85.76%; mp = 210–211 °C. IR ( $\nu_{\max}$ ,  $\text{cm}^{-1}$ ): 3221 (N–H), 3024 (N–H), 2956 (C–H), 1611 (C=N), 1582 (C=N), 1513 (C=C), 1477 (C–N). <sup>1</sup>H NMR (400 MHz)  $\delta$  (ppm): 7.90 (dd,  $J$  = 6.8 Hz, 1H, Ar–H), 7.73 (d,  $J$  = 7.2 Hz, 1H), 7.67 (d,  $J$  = 7.2 Hz, 1H, Ar–H), 7.65–7.62 (m, 2H, Ar–H), 7.28–7.16 (m, 4H, Ar–H), 6.92 (s, 1H, Ar–H), 6.81 (t,  $J$  = 7.6, 8.0 Hz, 3H, Ar–H), 6.74 (t,  $J$  = 7.2, 8.0 Hz, 1H, Ar–H), 3.42 (s, 3H), 1.85 (d,  $J$  = 6.4 Hz, 2H), 0.80 (t,  $J$  = 7.2 Hz, 2H). <sup>13</sup>C NMR (100 MHz)  $\delta$  (ppm): 147.4 (C), 147.0 (C), 144.1 (C), 143.4 (C), 143.0 (C), 132.3 (C), 131.5 (CH), 124.6 (CH), 122.0 (CH), 121.8 (CH), 118.8 (CH), 117.9 (C), 117.3 (C), 114.5 (CH), 113.9 (CH), 111.8 (CH), 110.8 (C), 74.7 (C), 71.6 (C), 33.2 (CH<sub>2</sub>), 27.6 (CH<sub>3</sub>), 7.9 (CH<sub>3</sub>). Anal. calcd. for C<sub>17</sub>H<sub>17</sub>N<sub>3</sub>: C, 77.54; H, 6.51; N, 15.96. Found: C, 77.38; H, 6.37; N, 15.81. GC–MS ( $m/z$ , M<sup>+</sup>): Found for C<sub>17</sub>H<sub>17</sub>N<sub>3</sub> = 263.15, expected mass = 263.14.

**9-Methyl-9-phenyl-8,10,17-triazatetracyclo[8.7.0<sup>2,7</sup>.0<sup>11,16</sup>]heptadeca-1(17),2,4,6,11(16),12,14-heptaene (III)**

2-(2'-Aminophenyl)-1*H*-benzimidazole (0.015 mol) was heated under reflux in acetophenone (10 mL) for 6 h. The

reaction mixture was allowed to stand for two weeks. The light yellow solid formed was filtered at the pump to obtain a yellow solid which recrystallized as yellow crystals from DMSO/toluene (1:1), yield = (2.39 g) 50.93%; mp = 124–125 °C. IR ( $\nu_{\max}$ ,  $\text{cm}^{-1}$ ): 3232 (N–H), 3006 (N–H), 2932 (C–H), 1611 (C=N), 1531 (C=C), 1505, 1492 (C–N). <sup>1</sup>H NMR (400 MHz)  $\delta$  (ppm): 7.95 (dd,  $J$  = 7.6, 8.0 Hz, 2H, Ar–H), 7.66–7.62 (m, 1H, Ar–H), 7.55–7.51 (m, 2H, Ar–H), 7.35 (s, 5H, Ar–H), 7.24 (t,  $J$  = 7.2, 8.4 Hz, 1H, Ar–H), 7.18 (t,  $J$  = 7.6 Hz, 1H, Ar–H), 7.03 (t,  $J$  = 7.2, 7.6 Hz, 1H, Ar–H), 6.95 (d,  $J$  = 8.0 Hz, 1H, Ar–H), 6.85 (d,  $J$  = 8.0 Hz, 1H, Ar–H), 6.81 (t,  $J$  = 7.6 Hz, 1H, Ar–H), 3.35 (s, 3H), 1.85 (s, 2H). <sup>13</sup>C NMR (100 MHz)  $\delta$  (ppm): 147.7 (C), 143.9 (C), 143.4 (C), 143.1, 136.8 (C), 133.2 (CH), 133.1 (CH), 131.6 (C), 128.7 (CH), 128.5 (CH), 128.1 (CH), 125.8 (C), 124.7 (CH), 122.1 (CH), 121.2 (CH), 118.9 (CH), 118.3 (CH), 114.7 (CH), 111.7 (CH), 74.8 (C), 26.8 (CH<sub>3</sub>). Anal. calcd. for C<sub>21</sub>H<sub>17</sub>N<sub>3</sub>: C, 81.00; H, 5.50; N, 13.49. Found: C, 80.93; H, 5.42; N, 13.30. LRMS ( $m/z$ , M<sup>+</sup>): Found for C<sub>21</sub>H<sub>17</sub>N<sub>3</sub> = 311.10, expected mass = 311.38.

**9-Methyl-9-propyl-8,10,17-triazatetracyclo[8.7.0<sup>2,7</sup>.0<sup>11,16</sup>]heptadeca-1(17),2,4,6,11(16),12,14-heptaene (IV)**

2-(2'-Aminophenyl)-1*H*-benzimidazole (0.015 mol) was heated under reflux in 2-pentanone (10 mL) for 6 h. The reaction mixture was allowed to stand overnight. The white solid formed was filtered at the pump and recrystallized as white crystals from THF/ethanol (1:1), yield = (2.56 g) 61.68%; mp = 165–166 °C. IR ( $\nu_{\max}$ ,  $\text{cm}^{-1}$ ): 3249 (N–H), 3110 (N–H), 2968 (C–H), 1610 (C=N), 1528 (C=C), 1481 (C–N). <sup>1</sup>H NMR (400 MHz)  $\delta$  (ppm): 7.92 (d,  $J$  = 7.6 Hz, 1H, Ar–H), 7.65 (d,  $J$  = 7.2 Hz, 2H, Ar–H), 7.23–7.15 (m, 3H, Ar–H), 6.81 (d,  $J$  = 8.4 Hz, 1H, Ar–H), 6.73 (t,  $J$  = 7.2, 7.6 Hz, 1H, Ar–H), 1.42–1.39 (br, 2H, CH<sub>2</sub>), 1.10–1.07 (br, 2H, CH<sub>2</sub>), 0.76 (t,  $J$  = 6.8, 7.2 Hz, 3H, CH<sub>3</sub>). <sup>13</sup>C NMR (100 MHz)  $\delta$  (ppm): 147.4 (C), 144.0 (C), 143.4 (C), 132.4 (CH), 131.6 (C), 128.8 (C), 128.1 (C), 125.2 (CH), 122.1 (CH), 121.8 (CH), 118.8 (CH), 117.3 (CH), 113.9 (CH), 111.8 (CH), 110.7 (C), 74.0 (C), 42.6 (CH<sub>2</sub>), 27.4 (CH<sub>3</sub>), 16.5 (CH<sub>2</sub>), 13.6 (CH<sub>3</sub>). Anal. calcd. for C<sub>18</sub>H<sub>19</sub>N<sub>3</sub>: C, 77.95; H, 6.90; N, 15.50. Found: C, 77.98; H, 6.75; N, 15.45. LRMS ( $m/z$ , M<sup>+</sup>): Found for C<sub>18</sub>H<sub>19</sub>N<sub>3</sub> = 277.65, expected mass = 277.36.

**9-Butyl-9-methyl-8,10,17-triazatetracyclo[8.7.0<sup>2,7</sup>.0<sup>11,16</sup>]heptadeca-1(17),2,4,6,11(16),12,14-heptaene (V)**

2-(2'-Aminophenyl)-1*H*-benzimidazole (0.015 mol) was heated under reflux in 2-hexanone (10 mL) for 6 h. The reaction mixture was allowed to stand overnight. The white solid

formed was filtered at the pump and recrystallized as white crystals from THF/ethanol (1:1). yield = (3.53 g) 80.75%; mp = 155–156 °C. IR ( $\nu_{\max}$ ,  $\text{cm}^{-1}$ ): 3222 (N–H), 3196 (N–H), 3106, 2957 (C–H), 2931 (C–H), 2870 (C–H), 1612 (C=N), 1530 (C=C), 1479 (C–N).  $^1\text{H}$  NMR (400 MHz)  $\delta$  (ppm): 7.91 (d,  $J=7.6$  Hz, 1H, Ar–H), 7.68–7.61 (m, 2H, Ar–H), 7.20–7.11 (m, 4H, Ar–H), 6.88 (s, 1H, Ar–H), 6.79 (d,  $J=8.0$  Hz, 1H, Ar–H), 6.73 (t,  $J=7.2$  Hz, 1H, Ar–H), 2.50 (s, 3H,  $\text{CH}_3$ ), 1.89–1.82 (m, 4H,  $2\text{CH}_2$ ), 1.09–1.00 (m, 2H,  $\text{CH}_2$ ), 0.72 (t,  $J=6.8, 7.2$  Hz, 3H,  $\text{CH}_3$ ).  $^{13}\text{C}$  NMR (100 MHz)  $\delta$  (ppm): 147.4 (C), 144.0 (C), 143.3 (C), 137.3 (C), 132.3 (C), 131.6 (CH), 128.8 (CH), 128.1 (CH), 125.2 (CH), 124.6 (CH), 122.1 (CH), 121.8 (CH), 118.8 (CH), 117.3 (CH), 113.9 (CH), 111.8 (CH), 110.7 (C), 74.4 (C), 27.5 ( $\text{CH}_3$ ), 25.2 ( $\text{CH}_2$ ), 21.9 ( $\text{CH}_2$ ), 20.9 ( $\text{CH}_2$ ), 13.8 ( $\text{CH}_3$ ). Anal. calcd. for  $\text{C}_{19}\text{H}_{21}\text{N}_3$ : C, 78.32; H, 7.26; N, 14.42. Found: C, 78.58; H, 7.38; N, 14.30. LRMS ( $m/z$ ,  $\text{M}^+$ ): Found for  $\text{C}_{19}\text{H}_{21}\text{N}_3 = 291.40$ , expected mass = 291.39.

**9-(propan-2-yl)-8,10,17-triazatetracyclo[8.7.0.0<sup>2,7</sup>.0<sup>11,16</sup>]heptadeca-(17),2,4,6,11(16),12,14-heptaene (VI)**

2-(2'-Aminophenyl)-1H-benzimidazole (0.015 mol) was heated under reflux with isobutyraldehyde (0.015 mol) in THF (15 mL) for 12 h. The solvent was removed at the pump to obtain a white solid which was recrystallized as a white crystal from ethanol/THF (1:1), yield = (3.71 g) 94%; mp = 192–193 °C. IR ( $\nu_{\max}$ ,  $\text{cm}^{-1}$ ): 3378 (N–H), 3172 (N–H), 1610 (C=N), 1520 (C=C), 1479 (C–N).  $^1\text{H}$  NMR (400 MHz)  $\delta$  (ppm): 12.67 (s, 1H), 7.93 (d,  $J=7.2$  Hz, 1H, Ar–H), 7.69–7.60 (m, 2H, Ar–H), 7.25–7.14 (m, 6H, Ar–H), 6.88 (s, 1H, Ar–H), 6.81 (d,  $J=8.0$  Hz, 2H, Ar–H), 6.73 (t,  $J=7.2, 7.6$  Hz, Ar–H) 1.84 (s, 6H,  $2\text{CH}_3$ ).  $^{13}\text{C}$  NMR (100 MHz)  $\delta$  (ppm): 152.5 (C), 148.2 (C), 147.0 (C), 144.1 (C), 143.0 (C), 133.5 (C), 132.3 (C), 131.5 (CH), 130.3 (CH), 127.2 (CH), 124.7 (CH), 122.3 (CH), 122.0 (CH), 121.8 (CH), 121.4 (CH), 118.8 (CH), 117.9 (CH), 116.1 (CH), 115.0 (CH), 114.5 (C), 111.9 (CH), 111.45 (C), 110.7 (CH) 110.1 (C), 71.9 (CH), 27.9 ( $\text{CH}_3$ ). Anal. calcd. for:  $\text{C}_{17}\text{H}_{17}\text{N}_3$ , C, 77.54; H, 6.51; N, 15.96. Found: C, 77.46; H, 6.42; N, 16.04. LRMS ( $m/z$ ,  $\text{M}^+$ ): Found for  $\text{C}_{17}\text{H}_{17}\text{N}_3 = 263.15$ , expected mass = 263.34.

**9-(3-Methylphenyl)-8,10,17-triazatetracyclo[8.7.0.0<sup>2,7</sup>.0<sup>11,16</sup>]heptadeca-(17),2,4,6,11(16),12,14-heptaene (VII)**

2-(2'-Aminophenyl)-1H-benzimidazole (0.015 mol) was heated under reflux with 4-methylbenzaldehyde (0.015 mol) in THF (15 mL) for 12 h. The solvent was removed at the pump to obtain a white solid which was recrystallized as a white crystal from ethanol/THF (1:1), yield = (4.48 g)

96%; mp = 203–204 °C. IR ( $\nu_{\max}$ ,  $\text{cm}^{-1}$ ): 3314 (N–H), 3041 (N–H), 2916 (C–H), 1616 (C=N), 1586 (C=C), 1528 (C=C), 1473 (C–N).  $^1\text{H}$  NMR (400 MHz)  $\delta$  (ppm): 7.97 (d,  $J=7.2$  Hz, Ar–H, 1H), 7.64 (d,  $J=8.0$  Hz, Ar–H, 1H), 7.54 (s, 1H, Ar–H), 7.25 (t,  $J=7.2, 7.6$  Hz, 1H, Ar–H), 7.20–7.07 (m, 7H, Ar–H), 7.01 (br, 1H, Ar–H), 6.85 (q, 2H), 2.22 (s, 3H).  $^{13}\text{C}$  NMR (100 MHz)  $\delta$  (ppm): 146.9 (C), 143.7 (C), 143.1 (C), 138.4 (C), 137.4 (C), 132.8 (C), 131.7 (C), 129.2 (CH), 125.8 (CH), 124.6 (CH), 122.2 (CH), 122.0 (CH), 118.6 (CH), 118.2 (CH), 114.8 (CH), 111.8 (C), 110.5 (CH), 67.7 (CH), 20.6 ( $\text{CH}_3$ ). Anal. calcd. for  $\text{C}_{21}\text{H}_{17}\text{N}_3$ : C, 81.00; H, 5.50; N, 13.49. Found: C, 80.94; H, 5.45; N, 13.33. LRMS ( $m/z$ ,  $\text{M}^+$ ): Found for  $\text{C}_{21}\text{H}_{17}\text{N}_3 = 311.10$ , expected mass = 311.14.

**9-Phenyl-8,10,17-triazatetracyclo[8.7.0.0<sup>2,7</sup>.0<sup>11,16</sup>]heptadeca-(17),2,4,6,11(16),12,14-heptaene (VIII)**

2-(2'-Aminophenyl)-1H-benzimidazole (0.015 mol) was refluxed with benzaldehyde (0.015 mol) in THF (15 mL) for 12 h. The solvent was removed at the pump to obtain a white solid which was recrystallized as a white crystal from ethanol/THF (1:1), yield = (4.37 g) 98%, mp = 210–211 °C. IR ( $\nu_{\max}$ ,  $\text{cm}^{-1}$ ): 3351 (N–H), 3056 (N–H), 1615 (C=N), 1582 (C=C), 1496 (C–N).  $^1\text{H}$  NMR (400 MHz)  $\delta$  (ppm): 7.98 (d,  $J=7.6$  Hz, 1H, Ar–H), 7.67 (d,  $J=7.6$  Hz, 1H, Ar–H), 7.62 (s, 1H, Ar–H), 7.31–7.24 (m, 6H, Ar–H), 7.21–7.14 (m, 2H, Ar–H), 7.13–7.07 (m, 2H, Ar–H), 6.89–6.82 (m, 2H, Ar–H).  $^{13}\text{C}$  NMR (100 MHz)  $\delta$  (ppm): 164.9 (C), 146.9 (C), 143.7 (C), 143.1 (C), 140.3 (C), 132.8 (C), 131.7 (CH), 128.9 (CH), 128.8 (CH), 125.9 (CH), 124.8 (CH), 122.3 (CH), 122.1 (CH), 118.6 (CH), 118.2 (CH), 114.8 (CH), 111.8 (C), 110.5 (CH), 67.8 (CH), 2.51 (CH). Anal. calcd. for  $\text{C}_{20}\text{H}_{15}\text{N}_3$ : C, 80.78; H, 5.08; N, 14.13. Found: C, 80.85; H, 5.15; N, 14.06. LRMS ( $m/z$ ,  $\text{M}^+$ ): Found for  $\text{C}_{20}\text{H}_{15}\text{N}_3 = 297.35$ , expected mass = 297.10.

**X-ray crystallography**

X-ray diffraction analyses of **I**, **III** and **VIII** were performed at 200 K using a Bruker Kappa Apex II diffractometer with monochromated Mo  $\text{K}\alpha$  radiation ( $\lambda = 0.71073 \text{ \AA}$ ). APEXII [29] was used for data collection and SAINT [29] for cell refinement and data reduction. The structures were solved by direct methods using SHELXS-2013, [30], and refined by least-squares procedures using SHELXL-2013 [31], with SHELXLE, as a graphical interface. All non-hydrogen atoms were refined anisotropically. Carbon-bound H atoms were placed in calculated positions (C–H 0.95 Å for aromatic carbon atoms and C–H 0.99 Å for methylene groups) and were included in the refinement in the riding model approximation, with Uiso (H) set to 1.2Ueq (C). The H atoms of the methyl groups were allowed to rotate with a fixed angle

around the C–C bond to best fit the experimental electron density (HFIX 137 in the SHELX program suite [29] with Uiso (H) set to 1.5Ueq (C). Nitrogen-bound H atoms were located on a difference Fourier map and refined freely. Data were corrected for absorption effects using the numerical method implemented in SADABS [29].

## Computational studies

The calculations were carried out using Gaussian 09 program. Molecular geometries of the singlet ground state of all the compounds were fully optimized in the gas phase at the density functional theory (DFT) using the B3LYP, CAM-B3LYP, B3PW91, WB97XD and M06 functionals and 6–311 g (d, p) basis set. An optimization and frequency calculation were carried out to ensure that the optimized molecular structure corresponded to a minimum. The results were viewed in Avogadro or Gaussview 6.0. The vibrational frequencies (IR), NMR and molecular electrostatic potentials of the compounds were also computed using the Gaussian 09 program.

## 2.DPPH assay

1,1-Diphenyl-2-picrylhydrazyl (DPPH) and ascorbic acid were purchased from Sigma–Aldrich (South Africa). A stock solution of DPPH (0.2 mM) was prepared in methanol. The solvents and other chemicals were of analytical grade. Compounds **I** to **VIII** ( $64$  to  $30 \times 10^{-6}$  mM) were tested for DPPH scavenging activity. Ascorbic acid ( $500$  to  $23 \times 10^{-8}$   $\mu$ M) was used as a positive control. Each compound (100  $\mu$ L) was added to a 96 well microtitre plate followed by the addition of 100  $\mu$ L DPPH (0.2 mM). Microtitre plates were wrapped in aluminium foil and kept in the dark at room temperature for 30 min. Spectrophotometric measurements completed at 517 nm using a BioTek Epoch 2 microtitre plate reader. The data were expressed as mean  $\pm$  SD for experiments completed out in triplicate. An average was obtained from the triplicate values for sample and blank; the blank was subtracted from all samples. The % DPPH scavenging =  $((\text{Abs DPPH} - \text{Abs Sample}) / (\text{Abs DPPH})) * 100$ . Prism software was

used to plot the % DPPH scavenging against the log of concentration, and the  $\text{IC}_{50}$  values were obtained.

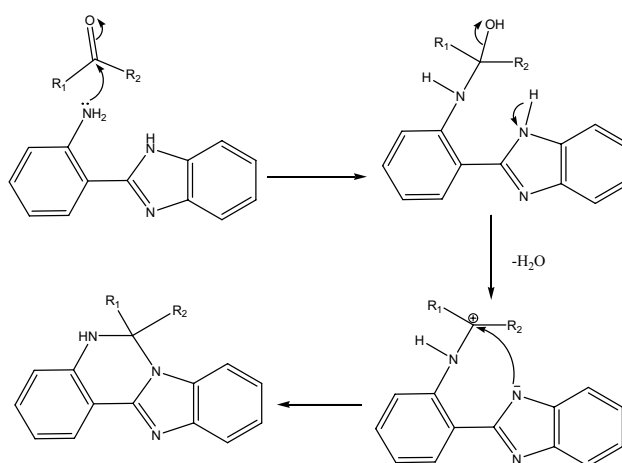
## Results and discussion

### Synthesis and characterization

The synthesis of some triazatetracyclics obtained from the condensation of aldehydes or ketones with 2-(2'-aminophenyl)-1*H*-benzimidazole as shown in Scheme 1.

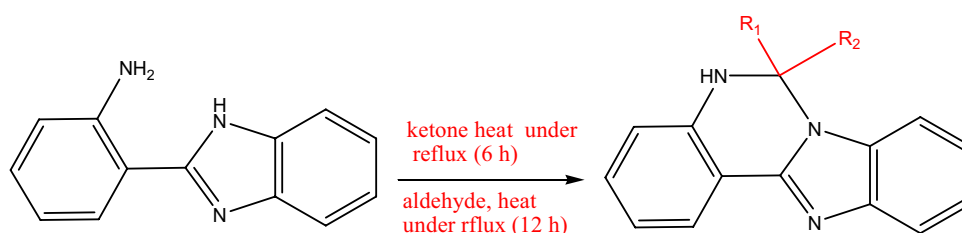
The reaction is proposed to proceed by the attack of the carbonyl of the ketone or aldehyde by the lone pair on the nitrogen of the 2-aminophenyl group leading to the formation of a hydroxyl group on the ketone or aldehyde (Scheme 2). The loss of the benzimidazole proton allows the carbanion formed to attack the carbonyl carbon leading to a loss of water and the formation of the triazatetracyclic compound.

The reaction leading to the formation of compounds **I–V** was carried out by heating the ketone (10 mL), as the



**Scheme 2** Proposed reaction mechanism for the formation of triazatetracyclics from ketones and aldehydes with 2-(2'-aminophenyl)-1*H*-benzimidazole

**Scheme 1** Synthesis of triazatetracyclics from ketones or aldehydes with 2-(2'-aminophenyl)-1*H*-benzimidazole



$R_1 = \text{H}, \text{CH}_3$

$R_2 = \text{methyl, ethyl, propyl, phenyl, isopropyl, phenyl, 4-methylphenyl}$

carbonyl source, with 2-(2'-aminophenyl)-1*H*-benzimidazole (0.015 mol). All products were characterized using IR,  $^1\text{H}$  NMR,  $^{13}\text{C}$  NMR, microanalysis and mass spectra. The NMR spectroscopic analysis confirmed the attachment of six methyl protons on the aminophenyl group at 2.00 ppm (6H, s) in the  $^1\text{H}$  NMR spectrum. Compound **I** has been synthesized by the slow evaporation of 2-(2'-aminophenyl)-1*H*-benzimidazole and acetone at room temperature for four days [32]. However, our method decreases the reaction time. The product was further unambiguously characterized by single-crystal X-ray diffraction analysis (Fig. 1).

In the synthesis of compound **II**, 2-butanone was used as a carbonyl source. The presence of two different sets of methyl protons at 0.80 (3H, t) and 3.42 ppm (3H, s) in the  $^1\text{H}$  NMR spectrum showed the attachment of 2-butanone to the aminophenylbenzimidazole. The attachment of the methyl groups was confirmed in the  $^{13}\text{C}$  NMR spectrum at 7.9 ( $\text{CH}_3$ ) and 27.6 ppm ( $\text{CH}_3$ ). The loss of the carbonyl of the ketone was confirmed by its absence in the  $^{13}\text{C}$  NMR spectrum. The presence of the methylene group was confirmed in the DEPT spectrum at 33.0 ppm ( $\text{CH}_2$ ). The formation of a carbocation in the proposed reaction mechanism (Scheme 2) suggests that the ketone would form a more stable carbocation, hence would give a better yield than the aldehydes. It was, however, observed that the aldehydes gave better yields than the ketones because the excess ketones used were not completely removed from the mother liquor upon completion of the reaction, making it difficult for the product to precipitate out. In the case of the aldehydes, equimolar quantities of reactants were used, and the reagents were dissolved in THF which was easily removed after the reaction, followed by re-crystallization to yield 94–98% products. Perhaps, a different work-up procedure might have resulted in better yields for the ketones, but solvent removal (in the case of ketones, excess reagent) followed by re-crystallization provided an easier purification route. A method for the synthesis of a compound similar to compound **V** but without the methyl

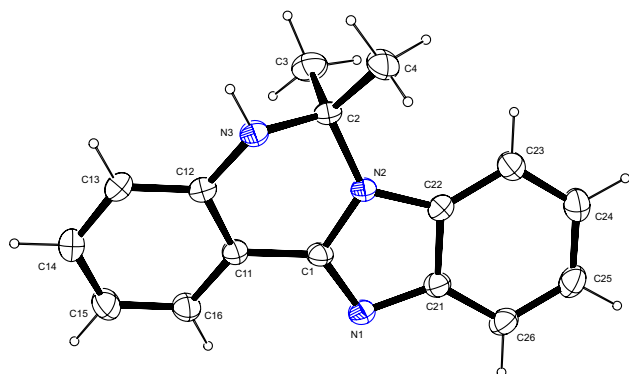


**Fig. 1** An ORTEP view of compound **1** showing 50% probability displacement ellipsoids and the atom labelling

group has been synthesized by heating *o*-aminophenylbenzimidazole and valeraldehyde in ethanol under reflux for 5 h [33]. The presence of methyl protons at 2.24 ppm (3H, s) in compound **III** was confirmed in the  $^1\text{H}$  NMR spectrum. The presence of a methyl group was also confirmed at 26.1 ppm in the  $^{13}\text{C}$  NMR spectrum.

The signals at 1.41 (2H, m) and 1.09 ppm (2H, m) confirmed the presence of two sets of methylene protons in the  $^1\text{H}$  NMR spectrum of compound **IV**. This was also confirmed in the DEPT and  $^{13}\text{C}$  NMR spectra by the signals at 42.6 ( $\text{CH}_2$ ) and 16.5 ppm ( $\text{CH}_2$ ). Two methyl protons were also observed at 0.76 ppm (6H, m) in the  $^1\text{H}$  NMR spectrum. The signals at 13.60 ( $\text{CH}_3$ ) and 2.74 ppm ( $\text{CH}_3$ ) in the DEPT and  $^{13}\text{C}$  NMR spectra confirmed the incorporation of the methyl groups in the structure.

The presence of three sets of methylene protons in compound **V** was confirmed by the signals at 1.86 (4H, m) and 1.08 (2H, m) ppm in the  $^1\text{H}$  NMR spectrum. The methylene groups occurred at 21.9 ( $\text{CH}_2$ ), 25.2 ( $\text{CH}_2$ ) and 40.0 ( $\text{CH}_2$ ) ppm in the  $^{13}\text{C}$  NMR and DEPT spectra. In the reaction of aldehydes with 2-(2'-aminophenyl)-1*H*-benzimidazole, THF was used as a solvent because 2-(2'-aminophenyl)-1*H*-benzimidazole was not soluble in the aldehydes; hence, the reaction could not be done using similar conditions used for the ketones.

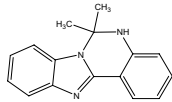
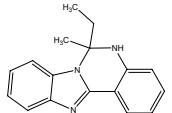
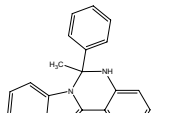
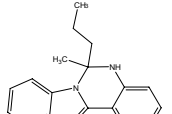
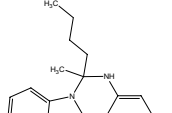
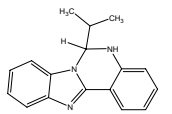
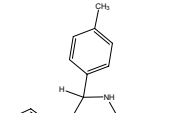
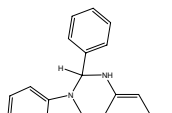
The presence of two methyl protons in the  $^1\text{H}$  NMR spectrum of compound **VI** was observed at 1.84 ppm (6H, s). The methyl groups were also confirmed in the  $^{13}\text{C}$  NMR and DEPT spectra at 27.9 ppm ( $\text{CH}_3$ ). The methyl protons on the phenyl ring occurred at 2.22 ppm ( $\text{CH}_3$ ) in the  $^1\text{H}$  NMR spectrum of compound **VII**, whilst the  $^{13}\text{C}$  NMR and DEPT spectra showed a methyl group at 20.6 ppm ( $\text{CH}_3$ ) and CH group at 67.7 ppm (CH) confirming the conversion of the  $sp^2$  carbon of the carbonyl to an  $sp^3$  carbon. The disappearance of the carbonyl signal in the  $^{13}\text{C}$  NMR of compound **VIII** confirmed the attachment of the aldehyde onto the aminophenylbenzimidazole. Also compound **VIII** and some of derivatives with substitution on the aryl ring have been synthesized from aminophenylbenzimidazole and substituted aryl aldehydes at room temperature in ethanol: acetic acid mixtures [35].

Table 1 gives the experimental conditions and yields of the synthesized compounds. Compound **VIII** has been synthesized by heating 2-(2'-aminophenyl) benzimidazole and an aryl aldehyde under reflux in ethanol for 5 h [34].

## Crystal structures

Compounds **I** and **III** were recrystallized from DMSO/toluene (1:1) as yellow crystals, whilst compound **VIII** was recrystallized from ethanol/THF (1:1) as white crystals. The crystallographic data, selected bond lengths and bond angles for the structures of compounds **I**, **III** and **VIII** are

**Table 1** Scope and yields of substituted triazetetrayclics

Entry	R <sup>1</sup>	R <sup>2</sup>	Solvent	Product	Reaction Tim (h)	Yields (%)
I	CH <sub>3</sub>	CH <sub>3</sub>	None		6	77
II	CH <sub>3</sub>	C <sub>2</sub> H <sub>5</sub>	None		6	86
III	CH <sub>3</sub>	C <sub>6</sub> H <sub>5</sub>	None		6	51
IV	CH <sub>3</sub>	C <sub>3</sub> H <sub>7</sub>	None		6	62
V	CH <sub>3</sub>	C <sub>4</sub> H <sub>9</sub>	None		6	81
VI	H	CHC <sub>2</sub> H <sub>6</sub>	THF		12	94
VII	H	4-CH <sub>3</sub> C <sub>6</sub> H <sub>4</sub>	THF		12	96
VIII	H	C <sub>6</sub> H <sub>5</sub>	THF		12	98

provided in Table S1. Compounds **I** and **III** crystallized in the monoclinic space group  $P2_1/c$ , whilst compound **VIII** crystallized in the monoclinic space group  $P2_1/n$ . The ORTEP diagram of compound **I** is presented in Fig. 1. The bond distance of N1–C1 was 1.317 (1) Å in compound **I**, 1.320(1), and 1.369(2) Å in compounds **III** and **VIII**, respectively, whilst the bond distance of N2–C1 was 1.374(1), 1.377(1) and 1.320(3) in compounds **I**, **III** and **VIII**, respectively. The bond lengths in the six membered ring of N3–C2–N2–C1–C11–C12 are not distinctly single nor double bonds with the bond lengths between 1.317(1) and 1.484(1), suggesting that the ring is further stabilized

by some degree of delocalization of electrons over the whole ring. The bond angle of C1–N1–C21 was 104.5(1), 104.4(1) and 124.2(2) in compounds **I**, **III** and **VIII**, respectively. The large deviation of the bond angle in compound **VIII** is due to the presence of the hydrogen which is sterically labile. The C2 carbon is  $sp^3$  hybridized and this decides the shape of the N3–C2–N2–C1–C11–C12 six membered ring. The hybridization of the C2 carbon makes the six membered ring to deviate from planarity. The ORTEP view of compounds **I**, **III** and **VIII** is given by Figs. 1, 2 and 3, respectively, showing 50% probability displacement ellipsoids and the atom labelling.

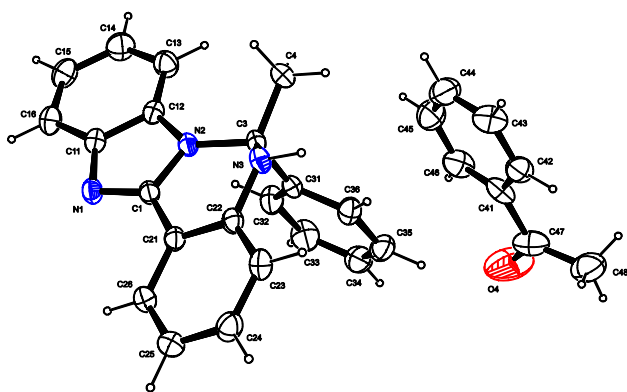


**Fig. 2** An ORTEP view of compound **III** showing 50% probability displacement ellipsoids and the atom labelling

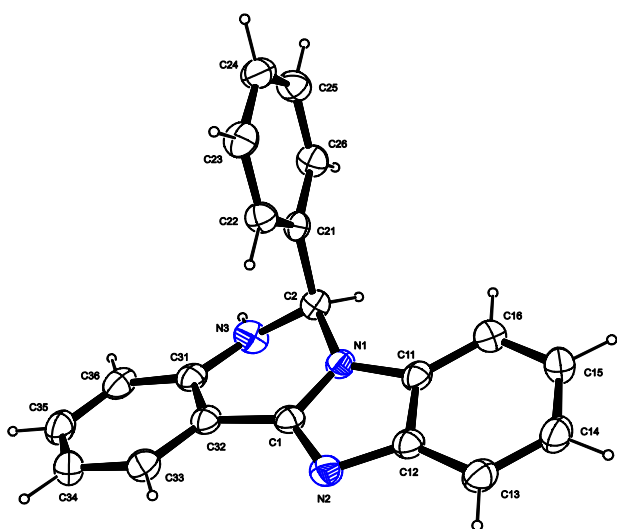


**Fig. 3** An ORTEP view of compound **VIII** showing 50% probability displacement ellipsoids and the atom labelling

### Comparison of theoretical and experimental bond parameters

Table 2 gives the summary of theoretical and experimental bond lengths and bond angles for compound **I** using B3LYP, CAM-B3LYP, B3PW91, WB97XD and M06 functionals and 6–311 g (d, p) basis set. The functionals and basis set were chosen based on previously reported work on the computation of triazatetracyclics [36–38]. The bond length of C25–C26 for compound **I** were experimentally determined as 1.381(2) Å, whilst the computed bond length gave deviations between 0.004 and 0.011 Å from the experimental values. For the amide bonds N1–C1, N2–C1, N2–C2 and N3–C12, the experimental bond lengths obtained were 1.317(1), 1.374(1), 1.476(1) and 1.382(2) Å, respectively, the computed values deviated by

0.003 and 0.018 Å from the experimental values. The bond lengths of C2–C4, C2–C3 and C11–C12 were experimentally determined as 1.520(2), 1.530(2) and 1.403(1) Å, whilst the computed values gave deviations between 0.001 and 0.013 Å. The bond lengths of C1–C11 and N1–C21 were experimentally determined as 1.450(1) and 1.387(1) Å with deviations of 0.001 to 0.004 and 0.001 to 0.013 Å representing the lowest and largest deviations, respectively, from the experimental values. The bond angles of C1–N1–C21, C1–C2–N2 and C2–N2–C22 were experimentally determined as 104.5(1), 122.8(1) and 106.5(1)°, whilst the computed values gave deviations of between 0.3 and 1.4° from the experimental values. The bond angles of N1–C1–N2 and N2–C2–N3 were experimentally determined as 113.5(1) and 106.0(1)° with deviations between 0.1 and 0.4° for the computed values. The bond angles of N2–C2–C4 and C2–N3–C12 were experimentally determined as 111.7(1) and 119.3(1)° with deviations of 0.1 to 0.2 and 0.4 to 1.6° representing the lowest and largest deviations, respectively, from the experimental values.

Table 3 gives the summary of theoretical and experimental bond lengths and bond angles of compound **III** using B3LYP, CAM-B3LYP, B3PW91, WB97XD and M06 functionals and 6–311 g (d, p) basis set. The bond lengths of C25–C26 and C1–C21 for compound **III** were experimentally determined as 1.381(2) and 1.453(1) Å, whilst the computed bond length gave deviations between 0.001 and 0.014 Å from the experimental values. For the amide bonds N2–C1, N2–C11 and N2–C3, the experimental bond lengths obtained were 1.377(1), 1.393(1) and 1.484(2) Å, respectively, the computed values deviated by 0.002 and 0.020 Å from the experimental values. The bond lengths of C3–C4, C3–C31, C11–C12 and C12–C13 were experimentally determined as 1.525(2), 1.540(1), 1.409(2) and 1.397(1) Å, whilst the computed values gave deviations between 0.001 and 0.014 Å. The bond lengths of N1–C1 were experimentally determined as 1.393(1) Å with a deviation of 0.001 to 0.003 Å representing the lowest deviation, whilst the bond lengths of N1–C1 and N2–C12 were 1.320(1) and 1.393(1) Å with deviations of 0.002 to 0.018 Å representing the lowest and largest deviations, respectively, for the from the experimental values. The bond angles of C1–N1–C11, C1–N2–C3, C1–N2–C12 and C3–N2–C12 were experimentally determined as 104.4(1), 120.8(1), 106.7(1) and 132.2(1)° with the computed values giving deviations between 0.3 and 2.1°. The bond angles of N2–C2–N3 and C1–N2–C22 were experimentally determined as 113.5(1) and 106.5(1)°, whilst the computed values gave deviations of between 0.4 and 1.6°. The bond angles of N1–C1–N2 and C2–N3–C12 were experimentally determined as 105.0(1) and 119.3(1)° with deviations of 0.1 to 0.2 and 0.4 to 1.6° representing the lowest and largest deviations, respectively, for the computed values.

**Table 2** Summary of theoretical and experimental bond lengths and bond angles of (I) using B3LYP, CAM-B3LYP, B3PW91, WB97XD and M06 functionals and 6-311 g (d,p) basis set

Compound I								
Experimental	B3LYP	CAM-B3LYP	B3PW91	WB97XD	M06	Min Deviation	Max Deviation	
<i>Bond length (Å)</i>								
N1–C1	1.317(1)	1.312	1.303	1.310	1.305	1.305	0.005	0.014
N2–C1	1.374(1)	1.392	1.382	1.386	1.381	1.384	0.007	0.018
C22–C23	1.393(2)	1.399	1.393	1.397	1.395	1.393	0.002	0.006
N1–C21	1.387(1)	1.379	1.390	1.388	1.379	1.374	0.001	0.013
C23–C24	1.384(2)	1.388	1.381	1.385	1.383	1.382	0.001	0.004
C24–C25	1.396(2)	1.405	1.401	1.403	1.402	1.399	0.003	0.009
N2–C2	1.476(1)	1.479	1.472	1.472	1.469	1.469	0.003	0.007
C25–C26	1.381(2)	1.392	1.385	1.390	1.386	1.386	0.004	0.011
N2–C22	1.388(1)	1.394	1.390	1.375	1.388	1.388	0.006	0.013
N3–C2	1.458(1)	1.471	1.463	1.464	1.463	1.462	0.004	0.013
N3–C12	1.382(1)	1.393	1.390	1.388	1.391	1.388	0.006	0.008
C1–C11	1.450(1)	1.451	1.453	1.448	1.454	1.446	0.001	0.004
C2–C4	1.520(2)	1.533	1.525	1.527	1.526	1.518	0.002	0.013
C2–C3	1.530(2)	1.543	1.534	1.537	1.536	1.527	0.003	0.013
C11–C12	1.403(1)	1.408	1.410	1.406	1.400	1.402	0.001	0.007
<i>Bond Angles (°)</i>								
C1–N1–C21	104.5(1)	105.2	105.1	105.0	104.8	104.8	0.3	0.7
C1–N2–C2	122.8(1)	122.3	122.1	122.0	122.0	122.2	0.5	0.8
C1–N2–C22	106.5(1)	106.0	105.1	106.1	106.0	105.9	0.4	1.4
C2–N2–C22	130.3(1)	130.1	130.3	130.2	130.1	129.8	0.1	0.5
C2–N3–C12	119.3(1)	120.9	120.5	120.5	119.7	120.4	0.4	1.6
N1–C1–N2	113.5(1)	113.4	113.6	113.9	113.8	113.8	0.1	0.4
N1–C1–C11	127.8(1)	127.1	127.0	127.0	127.0	127.1	0.7	0.8
N2–C1–C11	118.8(1)	119.5	119.4	119.4	119.1	119.1	0.3	0.7
N2–C2–N3	106.0(1)	105.8	105.9	105.7	105.7	105.9	0.1	0.3
N2–C2–C3	108.8(1)	109.2	109.2	109.1	109.0	109.1	0.2	0.4
N2–C2–C4	111.7(1)	111.9	111.8	111.9	111.8	111.7	0.1	0.2
N3–C2–C3	111.9(1)	112.1	112.1	112.2	112.2	112.1	0.2	0.3
N3–C2–C4	106.8(1)	106.5	106.7	106.6	106.8	106.8	0.1	0.2
N3–C12–C13	121.6(1)	122.0	122.0	122.1	122.0	122.0	0.4	0.5
N3–C12–C11	119.1(1)	118.6	118.6	118.5	118.6	118.7	0.4	0.6

Table 4 gives the summary of theoretical and experimental bond lengths and bond angles of compound **VIII** using B3LYP, CAM-B3LYP, B3PW91, WB97XD and M06 functionals and 6-311 g(d,p) basis set. The bond lengths of C1–C32 and C2–C21 for compound **VIII** was experimentally determined as 1.455(1) and 1.524(1) Å, respectively, whilst the computed bond length gave deviations between 0.001 and 0.009 Å from the experimental values. For the amide bonds N2–C1, N1–C2, N1–C11 and N2–C12, the experimental bond lengths obtained were 1.320 (3), 1.459(2), 1.385(3) and 1.391(3) Å, respectively, the computed values deviated by 0.005 and 0.017 Å from the experimental values. The bond lengths of N1–C1 and C11–C12 were experimentally determined as 1.369(1) and 1.406(3) with deviations of 0.007 to 0.018 and 0.001 to 0.011 Å representing the largest

deviations from the computed values. The lowest deviation was obtained for the C22–C23 as 0.002 to 0.004 Å from the experimental bond length of 1.388(3) Å. The bond angles of C1–N1–C2, C1–N1–C11 and C2–N1–C11 were experimentally determined as 124.2(2), 107.1(2) and 128.6(2)°, whilst the computed values gave deviations of between 0.2 and 1.2° from the experimental values. The bond angles of N1–C1–N2 and N2–C2–N3 were experimentally determined as 113.4(2) and 106.4(1)° with the computed values giving deviations between 0.1 and 0.9° from the experimental values. The bond angles of N1–C11–C12 and N2–C12–C13 were experimentally determined as 104.4(2) and 129.6(2) with deviations of 0.2 to 0.3 and 0.3 to 0.4 Å representing the lowest deviations, respectively, from the experimental values. The largest deviation was observed in N3–C31–C36

**Table 3** Summary of theoretical and experimental bond lengths and bond angles of (**III**) using B3LYP, CAM-B3LYP, B3PW91, WB97XD and M06 functionals and 6-311 g(d,p) basis set

Compound III								
Experimental	B3LYP	CAM-B3LYP	B3PW91	WB97XD	M06	Min Deviation	Max Deviation	
<i>Bond length (Å)</i>								
N1–C1	1.320(1)	1.312	1.302	1.310	1.304	1.305	0.002	0.018
N2–C1	1.377(1)	1.393	1.383	1.387	1.382	1.385	0.005	0.016
C34–C35	1.381(2)	1.395	1.389	1.392	1.391	1.389	0.008	0.014
N1–C11	1.393(1)	1.395	1.391	1.390	1.388	1.388	0.002	0.005
C35–C36	1.386(2)	1.391	1.385	1.389	1.387	1.385	0.001	0.005
N2–C3	1.484(1)	1.474	1.466	1.467	1.464	1.465	0.010	0.020
N2–C12	1.393(1)	1.395	1.378	1.375	1.379	1.375	0.002	0.018
N3–C3	1.460(1)	1.476	1.466	1.469	1.465	1.463	0.003	0.016
N3–C22	1.393(1)	1.395	1.392	1.390	1.394	1.391	0.001	0.003
C1–C21	1.453(1)	1.450	1.452	1.447	1.454	1.447	0.001	0.006
C3–C4	1.525(2)	1.537	1.529	1.531	1.529	1.520	0.004	0.012
C3–C31	1.540(1)	1.548	1.541	1.542	1.541	1.535	0.001	0.005
C11–C12	1.409(2)	1.419	1.409	1.417	1.411	1.413	0.002	0.010
C12–C13	1.397(2)	1.399	1.394	1.397	1.395	1.393	0.002	0.004
<i>Bond Angles (°)</i>								
C1–N1–C11	104.4(1)	105.3	105.1	105.1	104.8	104.8	0.4	0.9
C1–N2–C3	120.6(1)	122.7	122.3	122.5	121.6	120.9	0.3	2.1
C1–N2–C12	106.7(1)	106.1	106.0	106.2	106.1	106.0	0.5	0.7
N3–C22–C23	122.4(1)	122.0	122.1	122.1	122.3	122.4	0.1	0.4
C3–N2–C12	132.2(1)	130.3	130.7	130.4	130.8	131.3	0.9	1.9
N3–C22–C21	118.0(1)	118.5	118.4	118.4	118.2	118.2	0.2	0.5
C3–N3–C22	116.7(1)	120.5	119.8	120.2	118.4	117.9	1.2	3.8
N1–C1–N2	113.5(1)	113.3	113.5	113.4	113.7	113.7	0.1	0.2
N1–C1–C21	127.7(1)	127.1	127.1	127.1	127.2	127.5	0.2	0.6
N2–C1–C21	118.8(1)	119.6	119.3	119.5	119.0	118.8	0.5	0.8
N2–C3–N3	105.0(1)	105.6	105.7	105.7	105.4	105.0	0.4	0.7
N2–C3–C4	111.9(1)	110.9	110.6	111.1	111.3	111.5	0.4	1.0
N2–C3–C31	109.6(1)	111.1	110.9	109.9	110.5	110.5	0.9	1.5
N3–C3–C4	107.8(1)	106.2	106.4	106.3	106.9	107.2	0.6	1.6
N3–C3–C31	112.4(1)	111.5	111.6	111.5	111.7	111.9	0.5	0.9

which gave a computed bond angle of 122.2° with deviations of 0.8 and 2.8° from the experimental value. The M06 functional gave values closest to the experimental values for the bond lengths and bond angles of compounds **I** and **III**. For compound **VIII**, none of the functionals gave values that were consistent with the experimental values.

### HOMO–LUMO analysis

In order to gain a better understanding of the trends in the DPPH activity of the triazatetracyclics, a computational study of the frontier orbitals that account for the reactivity of the triazatetracyclics and the availability of the proton for DPPH scavenging activity was carried out. The energies of frontier molecular orbitals, energy band gap

( $E_{\text{HOMO}}-E_{\text{LUMO}}$ ), electronegativity ( $\chi$ ), chemical potential ( $\mu$ ), global hardness ( $\eta$ ), global softness ( $S$ ) and global electrophilicity index ( $\omega$ ) all contribute to the reactivity of the molecule. It is found that stability of molecules related to hardness [39]. Electronegativity is the power of an atom in a molecule to attract electron to itself [40]. The electrophilicity index gives a measure of energy lowering due to highest electron transfer between donor and acceptor [41]. The electrophilicity is a descriptor of reactivity that allows a quantitative classification of the global electrophilic nature of a molecule within a relative scale. To understand the toxicity of various compounds in terms of their reactivity and site selectivity, the new reactivity quantity can be demonstrated [42, 43].

**Table 4** Summary of theoretical and experimental bond lengths and bond angles of (**VIII**) using B3LYP, CAM-B3LYP, B3PW91, WB97XD and M06 functionals and 6-311 g(d,p) basis set

Compound VIII								
Experimental	B3LYP	CAM-B3LYP	WB97XD	M06	Min Deviation	Max Deviation		
<b>Bond length (Å)</b>								
N1–C1	1.369(2)	1.387	1.377	1.381	1.376	1.381	0.007	0.018
N2–C1	1.320(3)	1.314	1.304	1.312	1.306	1.307	0.006	0.016
N1–C2	1.459(2)	1.454	1.447	1.448	1.445	1.442	0.005	0.017
N1–C11	1.385(3)	1.385	1.385	1.379	1.378	1.378	0.006	0.007
N2–C12	1.391(3)	1.383	1.382	1.378	1.383	1.379	0.008	0.012
N3–C31	1.381(3)	1.397	1.394	1.392	1.395	1.392	0.011	0.016
C1–C32	1.455(3)	1.451	1.451	1.448	1.454	1.446	0.001	0.009
C2–C21	1.524(3)	1.529	1.529	1.524	1.523	1.518	0.005	0.006
C11–C12	1.406(3)	1.417	1.417	1.415	1.407	1.409	0.001	0.011
C12–C13	1.396(3)	1.399	1.399	1.397	1.389	1.393	0.001	0.007
C13–C14	1.379(3)	1.390	1.390	1.387	1.390	1.387	0.008	0.011
C14–C15	1.399(3)	1.407	1.407	1.405	1.405	1.401	0.002	0.008
C15–C16	1.386(3)	1.392	1.392	1.389	1.386	1.386	0.003	0.006
C21–C26	1.388(3)	1.397	1.397	1.395	1.392	1.392	0.004	0.009
C22–C23	1.388(3)	1.392	1.392	1.390	1.388	1.388	0.002	0.004
<b>Bond Angles (°)</b>								
C1–N1–C2	124.2(2)	124.9	124.9	124.8	124.8	124.4	0.2	0.7
C1–N1–C11	107.1(2)	106.7	106.6	106.8	106.7	106.5	0.3	0.6
C2–N1–C11	128.6(2)	127.9	128.0	127.9	127.6	127.4	0.7	1.2
C1–N2–C12	104.1(2)	105.2	105.1	105.0	104.8	104.9	0.7	1.1
C2–N3–C31	121.3(2)	120.8	120.5	120.5	119.7	119.7	0.5	1.6
N1–C1–N2	113.4(2)	112.9	113.1	113.0	113.3	113.2	0.1	0.5
N3–C31–C36	122.2(2)	121.3	121.3	119.4	121.4	121.3	0.8	2.8
N1–C1–C32	118.4(2)	118.5	118.4	118.5	118.1	118.0	0.1	0.4
N2–C1–C32	128.1(2)	128.6	128.5	128.5	128.6	128.7	0.4	0.6
N1–C2–N3	106.4(2)	107.1	107.3	107.2	107.3	107.2	0.7	0.9
N1–C2–C21	112.2(2)	113.5	113.2	113.3	112.6	112.6	0.4	1.3
N3–C2–C21	114.2(2)	113.5	113.4	113.4	113.5	113.3	0.7	0.9
N1–C11–C12	104.4(2)	104.7	104.7	104.6	104.7	104.7	0.2	0.3
N2–C12–C13	129.6(2)	129.9	129.9	129.9	130.0	129.9	0.3	0.4
N2–C12–C11	111.0(2)	110.5	110.4	110.6	110.5	110.6	0.4	0.6

**Table 5** Summary of global reactivity descriptors for (**I**) using B3LYP, CAM-B3LYP, B3PW91, WB97XD and M06 functionals and 6-311++ g(d,p) basis set

Compound 1					
	B3LYP	CAM-B3LYP	B3PW91	WB97XD	M06
Electronegativity ( $\chi$ )	0.13044	-0.13261	0.13138	0.13149	0.13528
Chemical potential ( $\mu$ )	-0.13044	0.13261	-0.13138	-0.13149	-0.13528
Global hardness ( $\eta$ )	0.07815	0.12445	0.07868	0.14548	0.08451
Global softness (S)	0.03908	0.06223	0.03934	0.07274	0.04226
Global electrophilicity index ( $\omega$ )	0.0085	0.0088	0.00863	0.00865	0.00915

Tables 5, 6 and 7 give the summary of the global reactivity descriptors for compounds **I**, **III** and **VIII** using B3LYP, CAM-B3LYP, B3PW91, WB97XD and M06 functionals and 6-311++ g(d,p) basis set, whilst Tables S1–S3 give the

HOMO–LUMO energy levels for compounds **I**, **III** and **VII** using B3LYP, CAM-B3LYP, B3PW91, WB97XD and M06 functionals and 6-311++ g(d,p) basis set.

**Table 6** Summary of global reactivity descriptors for (**III**) using B3LYP, CAM-B3LYP, B3PW91, WB97XD and M06 functionals and 6–311++ g(d,p) basis set

Compound III					
	B3LYP	CAM-B3LYP	B3PW91	WB97XD	M06
Electronegativity ( $\chi$ )	0.13119	0.13348	0.13222	0.13263	0.13605
Chemical potential ( $\mu$ )	-0.13119	-0.13348	-0.13222	-0.13263	-0.13605
Global hardness ( $\eta$ )	0.07831	0.12471	0.0788	0.14588	0.08569
Global softness (S)	0.03915	0.06236	0.0394	0.07294	0.04284
Global electrophilicity index ( $\omega$ )	0.00861	0.00891	0.00874	0.0088	0.00926

**Table 7** Summary of global reactivity descriptors for (**VIII**) using B3LYP, CAM-B3LYP, B3PW91, WB97XD and M06 functionals and 6–311++ g(d,p) basis set

Compound VIII					
	B3LYP	CAM-B3LYP	B3PW91	WB97XD	M06
Electronegativity ( $\chi$ )	0.13219	0.13425	0.13326	0.13330	0.13585
Chemical potential ( $\mu$ )	-0.13219	-0.13425	-0.13326	-0.13330	-0.13585
Global hardness ( $\eta$ )	0.07763	0.12397	0.07809	0.14494	0.08547
Global softness (S)	0.03881	0.06199	0.03905	0.07247	0.04274
Global electrophilicity index ( $\omega$ )	0.00873	0.00901	0.00888	0.00889	0.00923

The computation of the HOMO–LUMO energy gaps showed that the triazatetracyclic compounds do not differ greatly from each other in terms of their softness, hardness, electronegativity, electrophilicity and chemical potential. The difference in the computed values depends on the functional used in the computation.

### Comparison of computed and experimental NMR data

The computed NMR deviated variably from the experimental values. Tables S4–S6 give a summary of theoretical and experimental  $^1\text{H}$ NMR and  $^{13}\text{C}$  NMR data of compounds **I**, **III** and **VIII** using B3LYP, CAM-B3LYP, B3PW91, WB97XD and M06 functionals and 6–311++ g(d,p) basis set. The computed  $^1\text{H}$  NMR values for compound **I** gave deviations between 0.40 and 49.0% with the computed  $^{13}\text{C}$  NMR spectra giving deviations between 0.52 and 25.0%. For compound **III**, the computed values deviated by between 0.13 to 15.0% for the  $^1\text{H}$  NMR spectra, whilst the  $^{13}\text{C}$  NMR spectra gave deviations between 0.075 and 11.0%. The computed  $^1\text{H}$  NMR values for compound **VIII** gave deviations between 0.14 and 12% with the computed  $^{13}\text{C}$  NMR spectra giving deviations between 0.08 and 15.0%.

### Comparison of computed and experimental IR data

Figures S1–S7 give the computed IR for compounds **I** to **VIII**. IR was computed for two values of each compound (with the exception of **I** where there was symmetric substitution of two methyl groups). It was observed that the

scaling factors for vibrational frequencies which gave the best match to experimental data were 0.935 (b3lyp/6–311++ g(d,p)), 0.927 (cam-b3lyp/6–311++ g(d,p)), 0.931 (b3pw91/6–311++ g(d,p)), 0.925 (wb97xd/6–311++ g(d,p)) and 0.938 (m06/6–311++ g(d,p)). These differ from reported values 0.967 (b3lyp/6–311G(d,p)), 0.963 (b3pw91/6–311G(d,p)) and 0.957 (wb97xd/6–311G(d,p)). The difference is attributed to (i) the difference in basis sets between reported values and this work, and (ii) the narrow distribution in functionality in this set of compounds as compared to literature scaling functions. It was also observed that whilst there was a good correlation between four of the basis sets, the b3lyp calculations consistently were shifted to lower values at regions of lower wavenumber. Figure 4 shows the calculated infrared spectra using all functionals over two conformations of compound **II**.

### Molecular electrostatic potential

The electrostatic potential did not differ significantly between the functionals. However, the differing conformations (with the bulkier group in either the axial or equatorial positions) result in what appears to be differing surface access to the most negative regions of the electrostatic potential. Where the bulkier group is equatorially spaced, this region of highest negativity is not as exposed. Tables S7–S14 give the molecular electrostatic potential for compound **I–VIII** using b3lyp, cam-b3lyp, b3pw91, wb97xd and m06. Figure 5 illustrates the difference for two conformations of **III**.

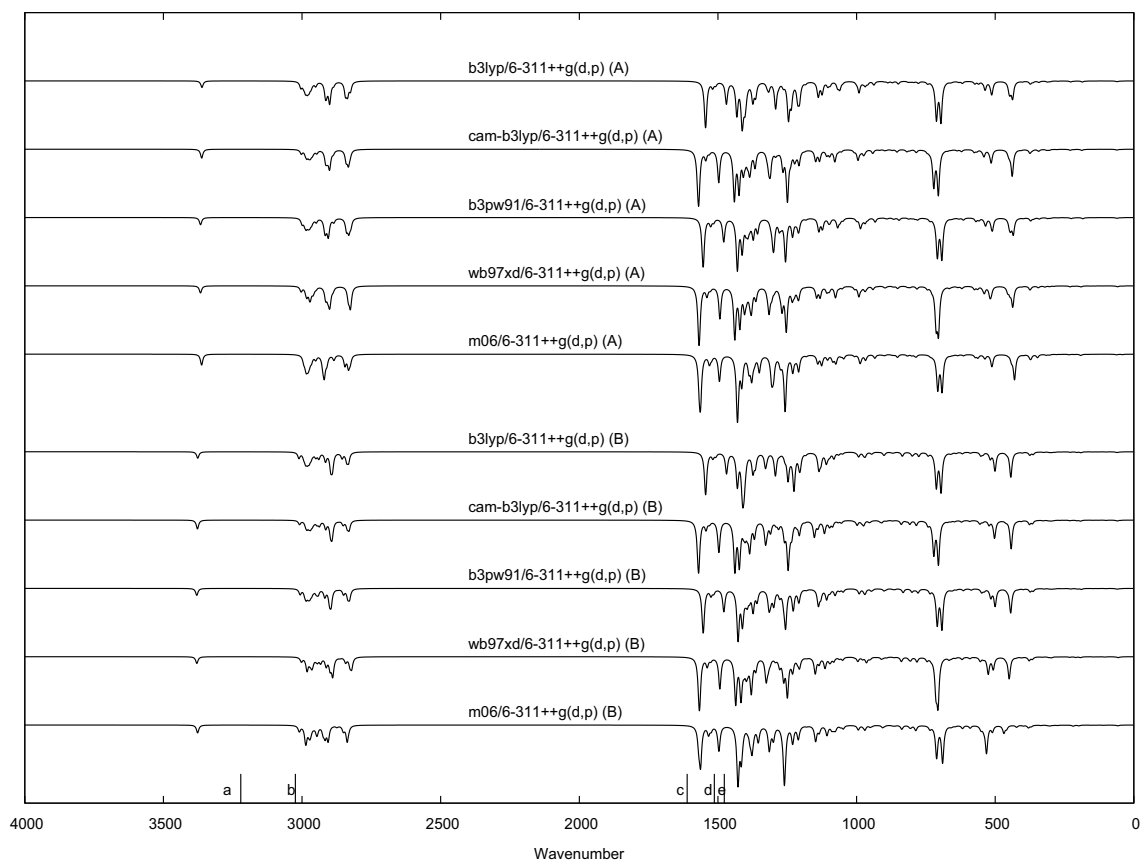
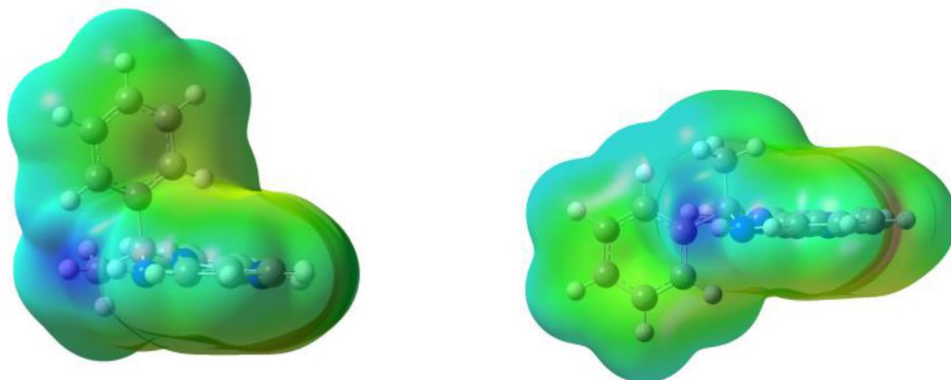


**Fig. 4** Plot of computed IR spectra for two conformations A and B of **II**. Key experimental bands at  $3221\text{ cm}^{-1}$  (a, N-H),  $3024\text{ cm}^{-1}$  (b, C-H),  $1611\text{ cm}^{-1}$  (c, C=N),  $1513\text{ cm}^{-1}$  (d, C=C) and  $1477\text{ cm}^{-1}$  (e, C-N) are shown as vertical markers

**Fig. 5** Molecular electrostatic potential for two conformations of **III** (with the bulkier phenyl group placed axially, left, and equatorially, right) calculated at the b3lyp/6-311++ g(d,p) level of theory

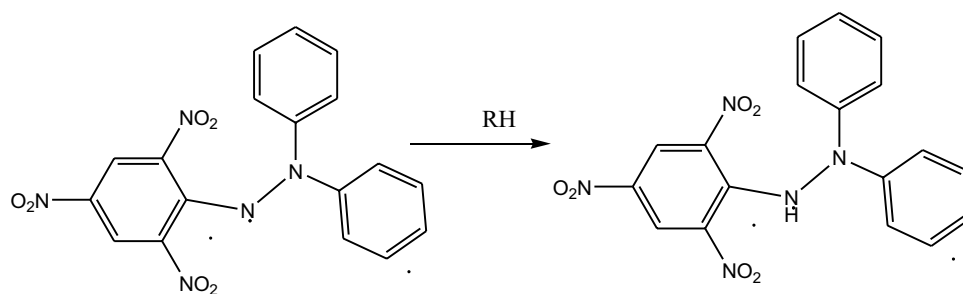


### DPPH scavenging activity

DPPH is a stable free radical that can accept an electron or hydrogen radical to become a stable diamagnetic molecule. Due to its odd electron, the methanolic solution of

DPPH shows a strong absorption band at 517 nm. DPPH radical reacts with various electron donating molecules (reducing agents or antioxidants). When electrons pair up, the DPPH solution becomes bleached. This results in the formation of the colourless 2,2'-diphenyl-1-picryl

**Scheme 3** The formation of the DPPH radical



hydrazine. Reduction of the DPPH radicals can be estimated quantitatively by measuring the decrease in absorbance at 517 nm [44]. Scheme 3 gives the formation of the DPPH radical. The activity of the compounds being tested was determined by their ability to easily contribute a proton to the DPPH radical.

In this set of tetrazatricyclic compounds, their scavenging activity was greatly influenced by the ease of loss of a proton. The higher activity of compound **I** is due to the accessibility of the proton by DPPH. The activity of the other derivatives was due to the presence of bulky groups obstructing DPPH's access to the proton. Table 4 gives the  $IC_{50}$  values for the scavenging activity of compounds

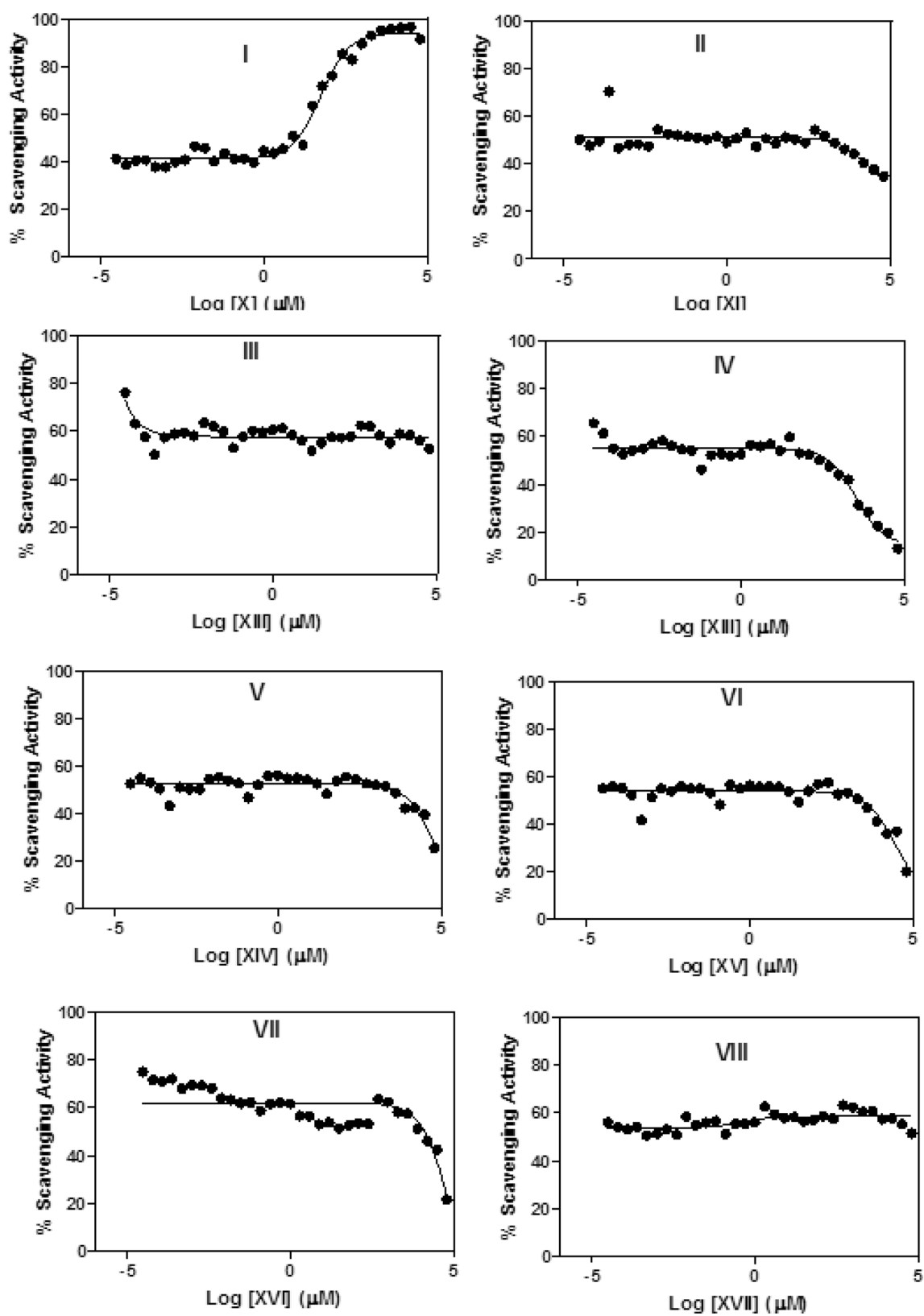
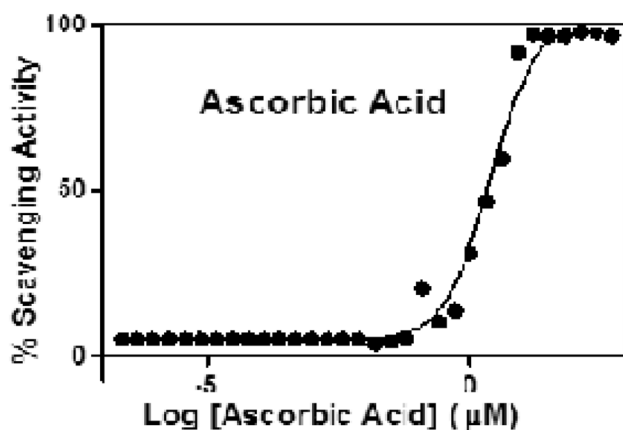


Fig. 6 A plot of percentage scavenging activity against log of concentrations of compounds I and VIII



**Fig. 7** A plot of percentage scavenging activity against log of concentrations of ascorbic acid

**Table 8** DPPH scavenging activity of compounds **I–VIII**

Compound	IC <sub>50</sub> (µM)
<b>I</b>	56.18
<b>II</b>	15,753
<b>III</b>	NC
<b>IV</b>	3321
<b>V</b>	68,830
<b>VI</b>	27,441
<b>VII</b>	89,491
<b>VIII</b>	0.3661
Ascorbic acid	2.365

**I–VIII** and ascorbic acid, whilst Figs. 6 and 7 give the plot of % scavenging activity against log of concentration for compounds **I–VIII** and ascorbic acid. Compound **I** exhibited a significant DPPH scavenging activity with an IC<sub>50</sub> of 56.18 µM compared to 2.37 µM for ascorbic acid (Table 8).

## Conclusion

In summary, we have confirmed the reactivity of 2-(2'-aminophenyl)-1*H*-benzimidazole with aldehydes and ketones, using the ketones both as solvents and reagents, and using THF for the aldehydes, to yield the triazatetracyclics. The compounds have been characterized using spectroscopy and microanalysis. The crystal structures of compounds **1**, **III** and **VIII** have been discussed. The computed IR and frontier molecular orbitals of the triazatetracyclics have been discussed. The computed bond lengths, bond angles, <sup>1</sup>H NMR and <sup>13</sup>C NMR of the compounds **I**, **III** and **VIII** have been discussed with experimental values; the molecular electrostatic potentials have been computed and the surface plotted for compounds **I–VIII**. The M06 functional gave

most of its values closest to the experimental values for the bond lengths and bond angles of compounds **I** and **III**. For compound **VIII**, none of the functionals gave values that were consistent with the experimental values. The 1,1-diphenyl-2-picrylhydrazyl (DPPH) scavenging activity of the triazatetracyclics showed that compound **I** exhibits significant DPPH scavenging activity with an IC<sub>50</sub> of 56.18 µM compared to 2.37 µM for ascorbic acid.

**Supplementary Information** The online version contains supplementary material available at <https://doi.org/10.1007/s13738-021-02158-3>.

**Acknowledgements** We thank MRC for the research funding (MRC-SIR). F. Odame thanks the National Research Foundation for awarding him a postdoctoral fellowship. We would also like to acknowledge the Center for High Performance Computing (CHPC) for allocation of resources (projects CHEM0802 and CHEM1261).

## Compliance with ethical standards

**Conflict of interest** The authors declare that they have no conflict of interest.

## References

- P.S. Hameed, A. Raichurkar, P.P. Madhavapeddi, S. Menasinakai, S.S. Sreevalli, P. Kaur, R. Nandishaiah, V. Panduga, R.J. Jitendar, V.K. Sambandmurthy, D. Sriram, A.C.S. Med. Chem. Lett. **5**, 820 (2014)
- A.J. Ndakala, R.K. Gessner, P.W. Gitrari, N. October, K.L. White, A. Hudson, F. Fakorede, D.M. Shackelford, M. Kaiser, C. Yeates, A. Susan, S.A. Charman, K. Chibale, J. Med. Chem. **54**, 4581 (2011)
- K. Kubo, Y. Inada, Y. Kohara, Y. Sugiura, M. Ojima, K. Itoh, Y. Furukawa, K. Nisikawo, T.J. Naka, J. Med. Chem. **36**, 1772 (1993)
- T. Roth, L.M. Morningstar, P.L. Boyer, S.H. Hughes, R.W. Buckheit, C.J. Michejda, J. Med. Chem. **40**, 4199 (1997)
- J.S. Kim, B. Gatto, C. Yu, L.F. Liu, E.L. Lavoie, J. Med. Chem. **39**, 992 (1996)
- G.D. Williams, R.A. Pike, Org. Lett. **22**, 4227 (2003)
- M.K. Jeganath, K. Pitchumani, A.C.S. Sustain, Chem. Eng. **2**, 1169 (2014)
- F. Odame, P. Kleyi, E. Hosten, R. Betz, K. Lobb, Z. Tshentu, Molecules **18**, 14293 (2013)
- Y. Kurosaki, K. Shirokane, T. Toishi, T. Sato, N. Chida, Org. Lett. **14**, 2098 (2012)
- G. K. Goering, Ph.D. Thesis, Cornell University, Ithaca (1995)
- T.M. Das, C.P. Rao, E. Kolehmainen, Carbohydr. Res. **334**, 261 (2001)
- Y.S. Chhonker, B. Veenu, S.R. Hasim, N. Kaushik, D. Kumar, P. Kumar, Eur. J. Chem. **6**, S342 (2009)
- H. Pessoa-Mahana, C.D. Pessoa-Mahana, R. Salazar, J.A. Valderrama, E. Saez, R. Araya-Maturana, Synthesis **3**, 436 (2004)
- M.A. Arafath, F. Adam, F.S.R. Al-Suede, M.R. Razali, M.B.K. Ahamed, A.M.S.A. Majid, M.Z. Hassan, H. Osman, S. Abubakar, J. Mol. Struct. **1149**, 216 (2017)
- R. Pandey, M. Yadav, M. Shahid, A. Misra, D.S. Pandey, Tetrahedron Lett. **53**(28), 3550 (2012)

16. A. Cardador-Martinez, G. Loacra-Pina, B.D. Oomah, J. Agric. Food Chem. **50**, 6975 (2002)
17. V.N. Enujiugha, In: R. Dris, Ed., Crops: Growth, Quality and Biotechnology, WFL Publisher, Helsinki, 732 (2005)
18. V.N. Enujiugha, O. Ayodele-Oni, Int. J. Food Sci. Tech. **38**, 525 (2003)
19. V.N. Enujiugha, Adv. Food Sci. **32**, 88 (2010)
20. S.A. Ordoudi, M.Z. Tsimidou, A.P. Vafiadis, E.G. Bakalbassis, J. Agric. Food Chem. **54**, 5763 (2006)
21. E.B. Solis, M. Flores-Alamo, D. Ramirez-Rosales, R. Zamorano-Ulloa, S. Hernandez-Anzaldo, Y. Reyes-Ortega, J. Anal. Bioanal. Tech. **7**, 315 (2016)
22. P. Jing, S.J. Zhao, W.J. Jian, J.B. Qian, Y. Dong, J. Pang, Molecules **17**, 12910 (2012)
23. C.H. Choi, M. Kertez, J. Phys. Chem. A **101**, 3823 (1997)
24. M. Kurt, P.C. Babu, N. Sundaraganesan, M. Cinar, M. Karabacak, Spectrochim. Acta A **79**, 1162 (2011)
25. D.F.V. Lewis, C. Ioannides, D.V. Parke, Xenobiotica **24**, 401 (1994)
26. L. Padmaja, R.C. Kunar, D. Sajan, I.H. Joe, V.S. Jayakumar, G.R. Pettit, O.F. Nielsen, J. Raman Spectrosc. **40**, 419 (2009)
27. A. Poiyamozi, N. Sundaraganesan, M. Karabacak, O. Tanriverdi, M. Kurt, J. Mol. Struct. **1024**, 1 (2012)
28. P. Udhayakala, A. Jayanthi, T.V. Rajendiran, S. Gunasekaran, Arch. Appl. Sci. Res. **3**, 424–439 (2011)
29. APEX2 SADABS and SAINT. Bruker AXS Inc: Madison, WI (2010)
30. G.M. Sheldrick, Acta. Cryst. A **64**, 112 (2008)
31. C.B. Hubschle, G.M. Sheldrick, B. Ditttrich, J. Appl. Cryst. **44**, 1281 (2011)
32. A. Esparza-Ruiz, A. Pena-Hueso, E. Mijanjos, G. Osorio-Monreal, H. Nöth, A. Flores-Parra, R.R. Contreras, N. Barba-Behrens, Polyhedron **30**, 2090 (2011)
33. S. Naveen, S.M. Anandalwar, J.S. Prasad, V. Gayathri, R. Bhattacharjee, Anal. Sci. **22**, 185–186 (2006)
34. P.P. Joshi, S.G. Shirodkar, WJPPS **3**, 950 (2014)
35. B.A. Insuasty, H. Torres, J. Quiroga, R. Abonia, R. Rodriguez, M. Nogerias, A. Sanchez, C. Saitz, S.L. Avarez, S.A. Zacchino, J. Child. Chem. Soc. **51**, 927 (2006)
36. F. Odame, E.C. Hosten, Acta Chim. Slov. **65**, 531 (2018)
37. F. Odame, E.C. Hosten, R. Betz, Z. Tshentu, J. Struct. Chem. **59**(8), 1804 (2018)
38. F. Odame, E.C. Hosten, Z.R. Tshentu, J. Struct. Chem. **61**(8), 1177 (2020)
39. P.G. Parr, P.K. Chattaraj, J. Am. Chem. Soc. **13**, 1854 (1991)
40. L. Pauling, *The Nature of the Chemical Bond*, 3rd edn. (Cornell University Press, Ithaca, 1960).
41. P.G. Parr, L. von Szentpaly, S. Liu, J. Am. Chem. Soc. **121**, 1922 (1999)
42. R. Parthasarathi, J. Padmanabhan, V. Subramanian, B. Maiti, P.K. Chattaraj, J. Phys. Chem. A **107**, 10346 (2003)
43. R. Parthasarathi, J. Padmanabhan, V. Subramanian, B. Maiti, P.K. Chattaraj, Curr. Sci. **86**, 535 (2004)
44. V. Venkatachalam, Y. Nayak, B.S. Jayashree, Int. J. Chem. Eng. Appl. **3**, 216 (2012)